

An Efficient Lactone-to-Lactam Conversion for the Synthesis of Thiophene Pechmann Lactam and Characterization of Polymers Thereof

Kyu Cheol Lee^{a,c,†}, Hae Rang Lee^{b,d,†}, So-Huei Kang^a, Jungho Lee^a, Young IL Park^c, Seung Man Noh^c, Joon Hak Oh^{b,}, and Changduk Yang^{a,*}*

^aDepartment of Energy Engineering, School of Energy and Chemical Engineering, Perovtronic Research Center, Low Dimensional Carbon Materials Center, Ulsan National Institute of Science and Technology (UNIST), 50 UNIST-gil, Ulju-gun, Ulsan 44919, South Korea. E-mail: yang@unist.ac.kr

^bSchool of Chemical and Biological Engineering, Institute of Chemical Processes, Seoul National University, 1, Gwanak-ro, Gwanak-gu, Seoul 08826, South Korea. E-mail: joonhoh@snu.ac.kr

^cResearch Center for Green Fine Chemicals, Korea Research Institute of Chemical Technology, Ulsan 44412, South Korea.

^dDepartment of Chemical Engineering, Pohang University of Science and Technology (POSTECH), Pohang, Gyeongbuk 37673, South Korea.

Table of Contents	Page
Fig. S1 ¹ H NMR (CDCl ₃ , 400 MHz) spectrum of compound 3 .	S3
Fig. S2 ¹³ C NMR (CDCl ₃ , 400 MHz) spectrum of compound 3 .	S4
Fig. S3 ¹ H NMR (CDCl ₃ , 400 MHz) spectrum of compound 4 .	S5
Fig. S4 ¹³ C NMR (CDCl ₃ , 100 MHz) spectrum of compound 4 .	S6
Fig. S5 ¹ H NMR (C ₂ D ₂ Cl ₄ at 80 °C, 600 MHz) spectrum of PTBPD-Th.	S7
Fig. S6 ¹ H NMR (C ₂ D ₂ Cl ₄ at 80 °C, 600 MHz) spectrum of PTBPD-Th2.	S8
Fig. S7 ¹ H NMR (C ₂ D ₂ Cl ₄ at 80 °C, 600 MHz) spectrum of PTBPD-Se.	S9
Fig. S8 ¹ H NMR (C ₂ D ₂ Cl ₄ at 80 °C, 600 MHz) spectrum of PTBPD-Se2	S10
Fig. S9 Cyclic voltammetry of TBDP-based polymers.	S11
Fig. S10 Energy level diagrams of TBDP-based polymers	S12
Fig. S11 DFT calculation for TBDP-based polymers at the B3LYP/6-31G* level.	S13
Fig. S12 AFM height images of TBPDP-based polymer films annealed at 200 °C: (a) PTBPD-Th, (b) PTBPD-Th2, (c) PTBPD-Se, and (d) PTBPD-Se2.	S14
Fig. S13 2D-GIXD images of TBPDP-based polymer films without thermal treatment: (a) PTBPD-Th, (b) PTBPD-Th2, (c) PTBPD-Se, and (d) PTBPD-Se2. The corresponding GIXD diffractogram profiles: (e) in-plane and (f) out-of-plane GIXD patterns.	S15
Table S1. Crystallographic parameters of TBPDP-based polymer films without thermal treatment.	S16
Table S2 Summary of FET performance of pristine TBPDP polymer films	S17
Fig. S14 Transfer characteristics obtained from TBPDP-based polymer films before (blue) and after thermal treatment at various annealing temperature of 150 °C (green), 200 °C (orange), and 250 °C (red): (a) PTBPD-Th, (b) PTBPD-Th2, (c) PTBPD-Se, and (d) PTBPD-Se2.	S18
Table S3. FET performance of TBPDP polymer films fabricated using various solvents.	S19
Fig. S15 Transfer curves with three fitting lines obtained from TBPDP-based polymer films after thermal treatment at 200 °C: (a) PTBPD-Th, (b) PTBPD-Th2, (c) PTBPD-Se, and (d) PTBPD-Se2. The red lines represent the fitting line of the maximum mobility. The green lines represent the fitting lines with high gate bias. The blue lines represent ideal FET characteristics (satisfying the ideal Shockley equations).	S20
Table S4. Summary of the calculated mobilities of TBPDP polymer-based OFETs.	S21
Fig. S16 Thermogravimetric analysis (TGA) of all polymers.	S22
Fig. S17 The differential scanning calorimetry (DSC) data of all polymers.	S23

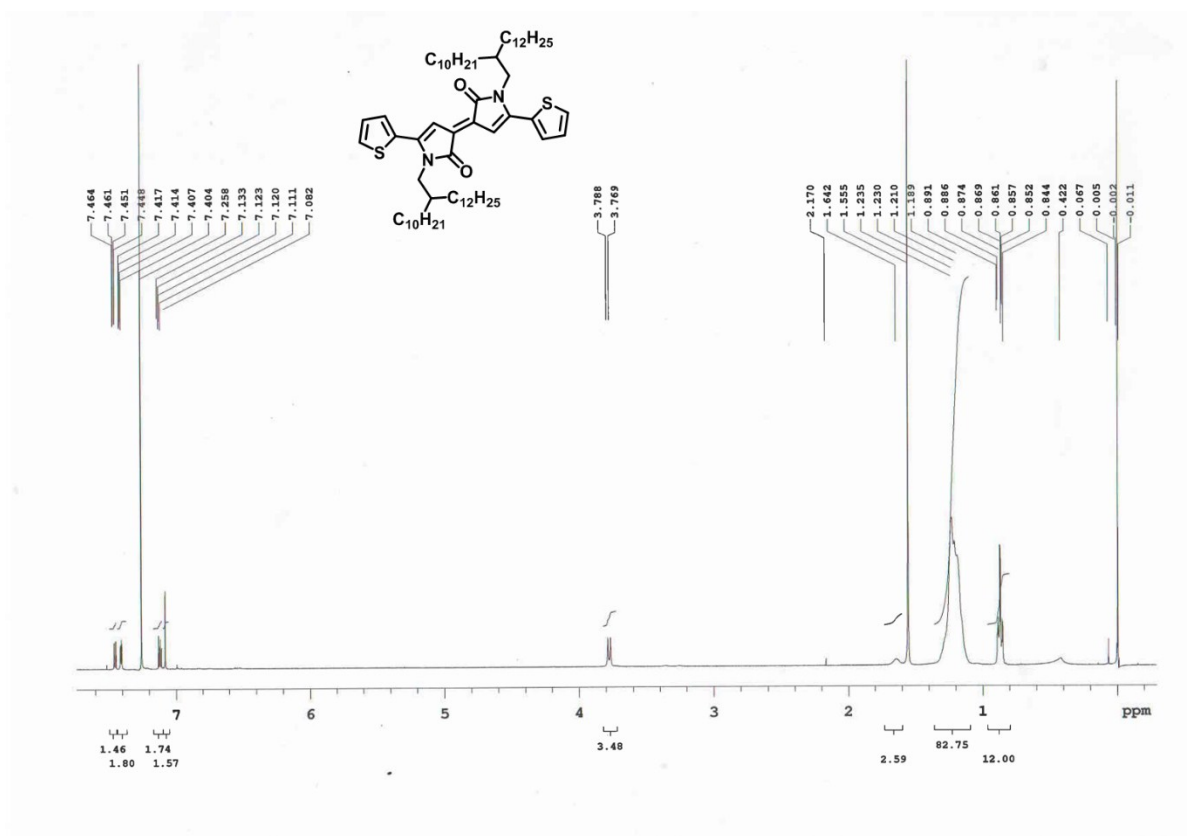


Fig. S1 ¹H NMR (CDCl₃, 400 MHz) spectrum of compound **3**.

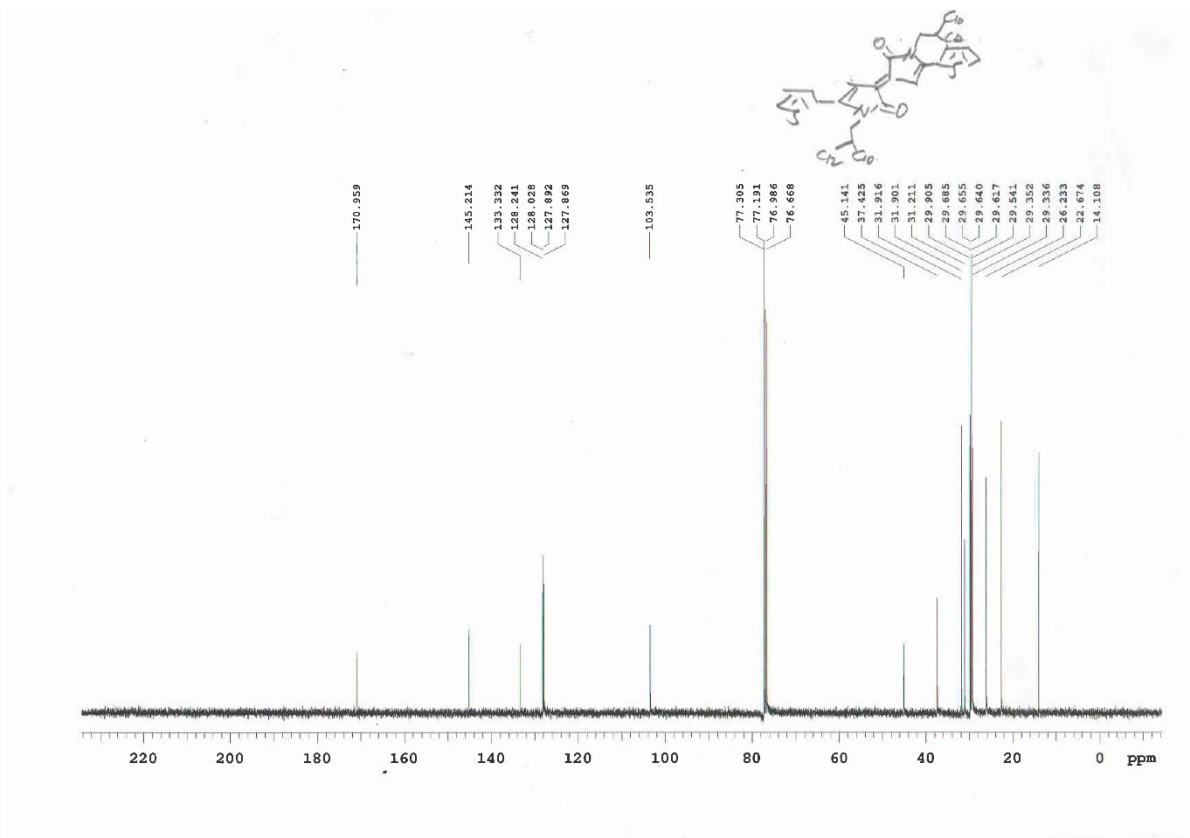


Fig. S2 ^{13}C NMR (CDCl_3 , 400 MHz) spectrum of compound 3.

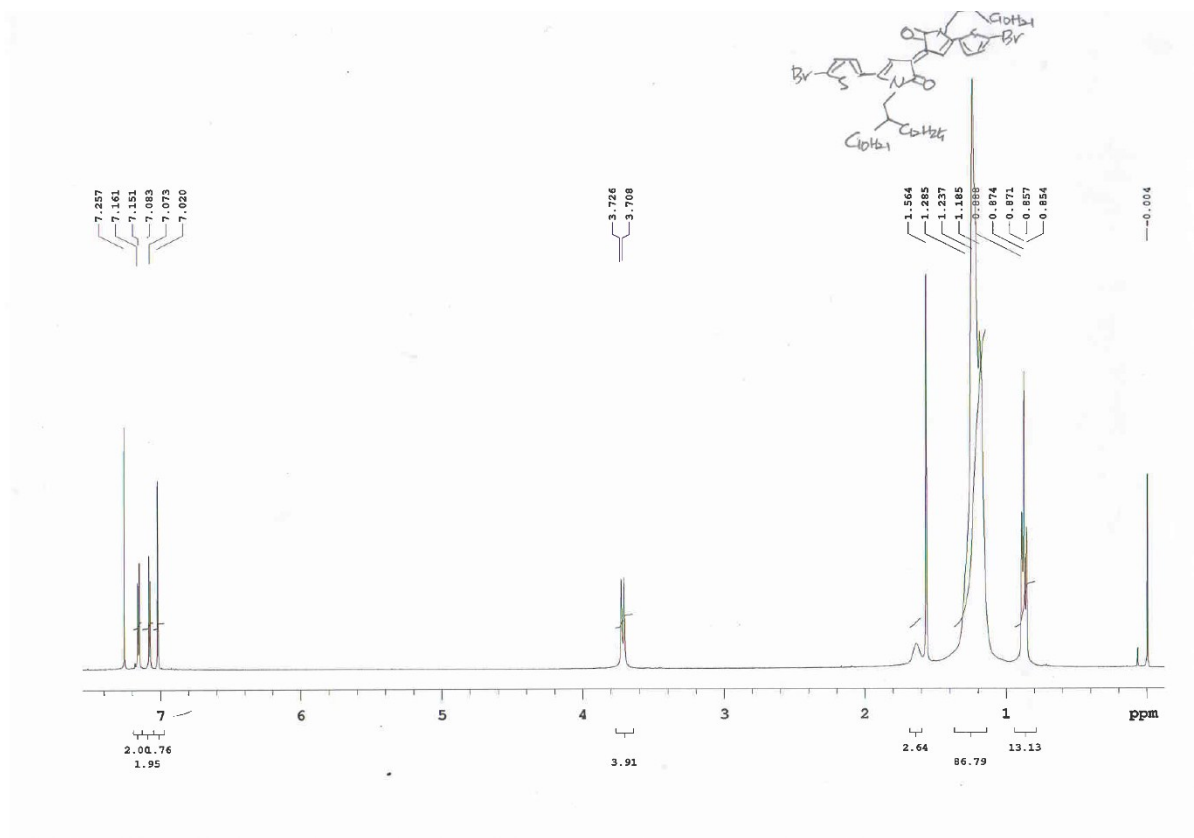


Fig. S3 ¹H NMR (CDCl₃, 400 MHz) spectrum of compound **4**.

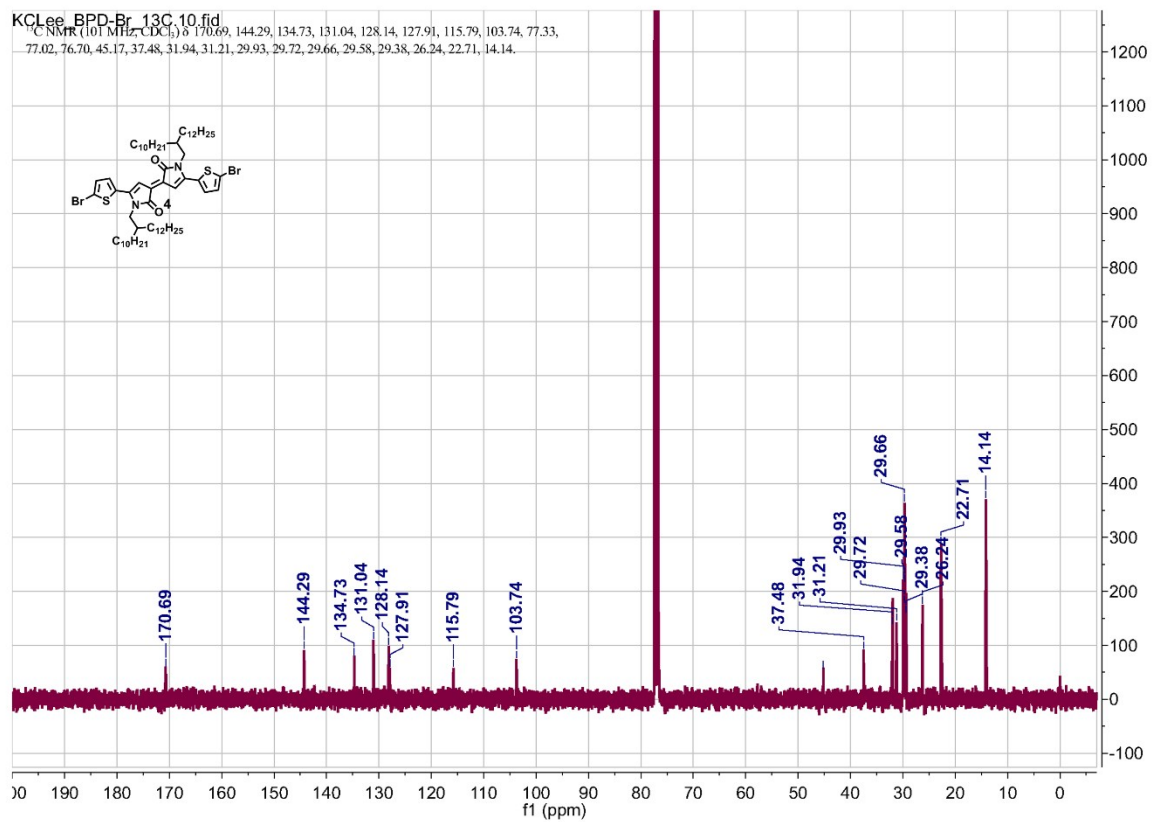


Fig. S4 ¹³C NMR (CDCl₃, 100 MHz) spectrum of compound 4.

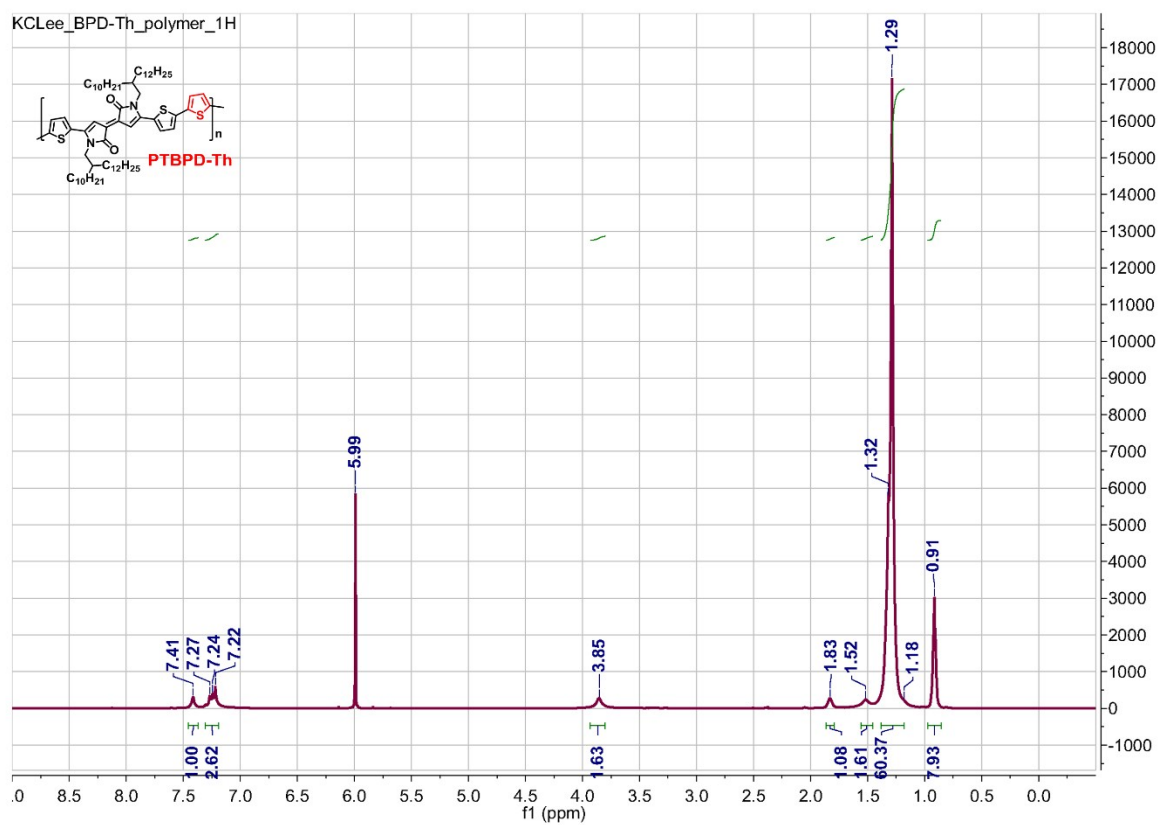


Fig. S5 ¹H NMR (C₂D₂Cl₄ at 80 °C, 600 MHz) spectrum of PTBPD-Th.

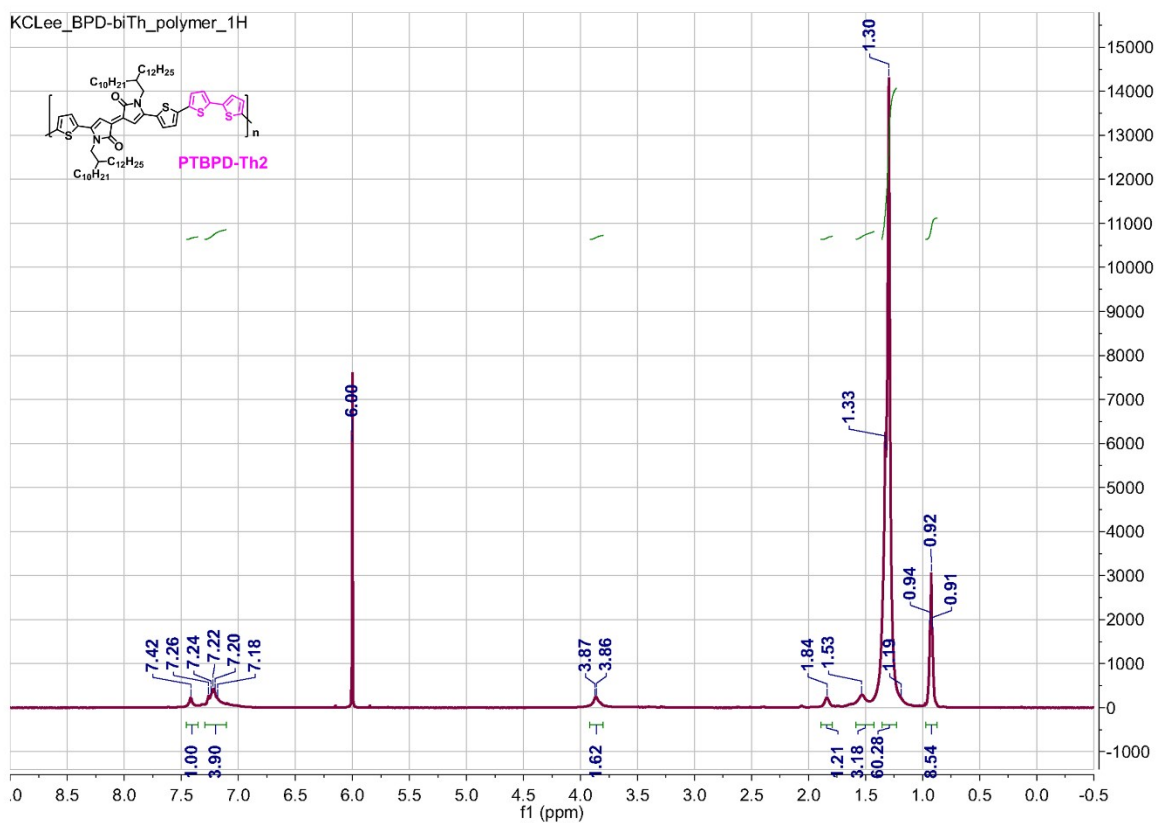


Fig. S6 ^1H NMR ($\text{C}_2\text{D}_2\text{Cl}_4$ at $80\text{ }^\circ\text{C}$, 600 MHz) spectrum of PTBPD-Th2.

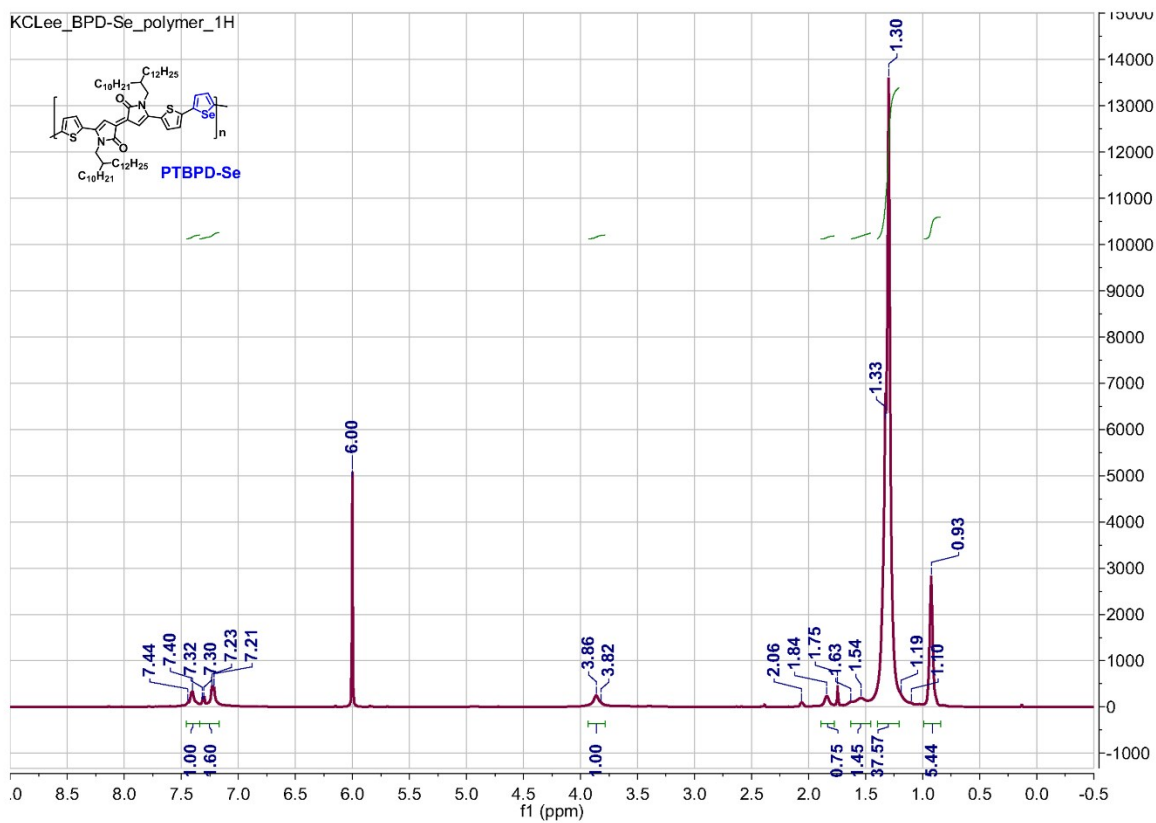


Fig. S7 ¹H NMR (C₂D₂Cl₄ at 80 °C, 600 MHz) spectrum of PTBPD-Se.

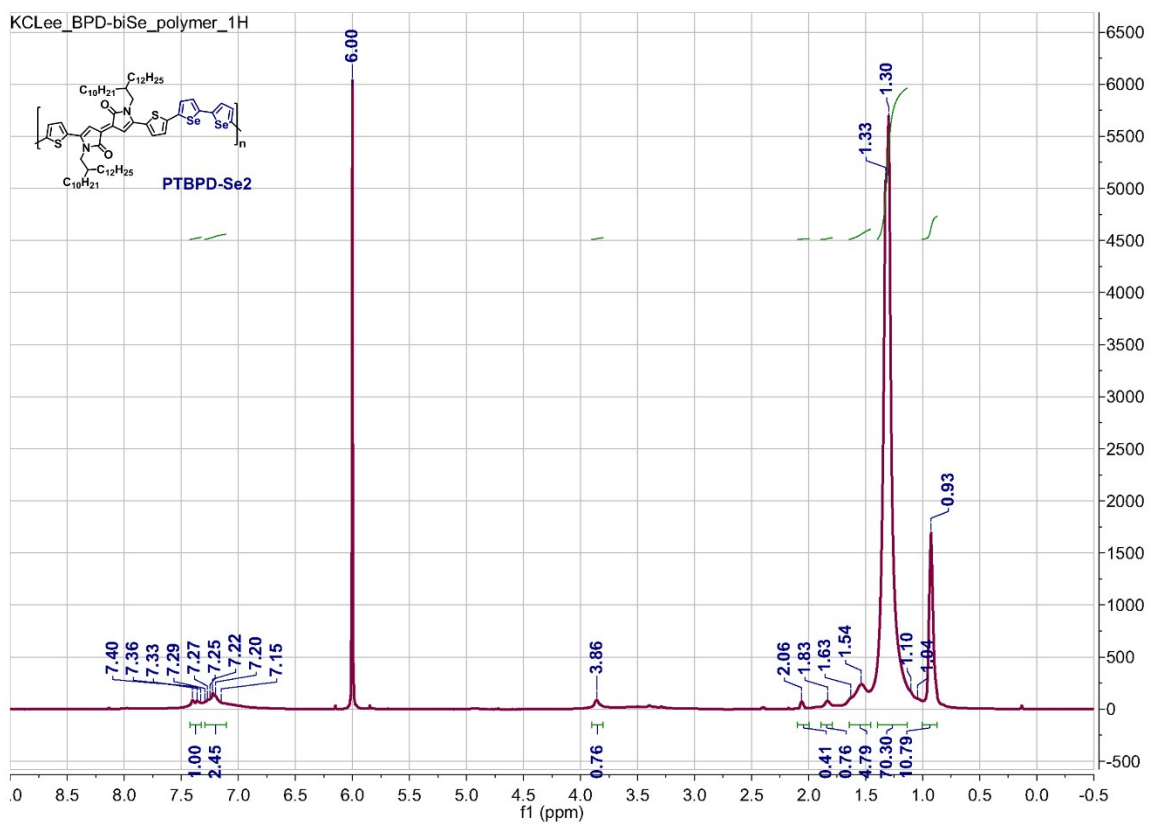


Fig. S8 ¹H NMR (C₂D₂Cl₄ at 80 °C, 600 MHz) spectrum of PTBPD-Se2.

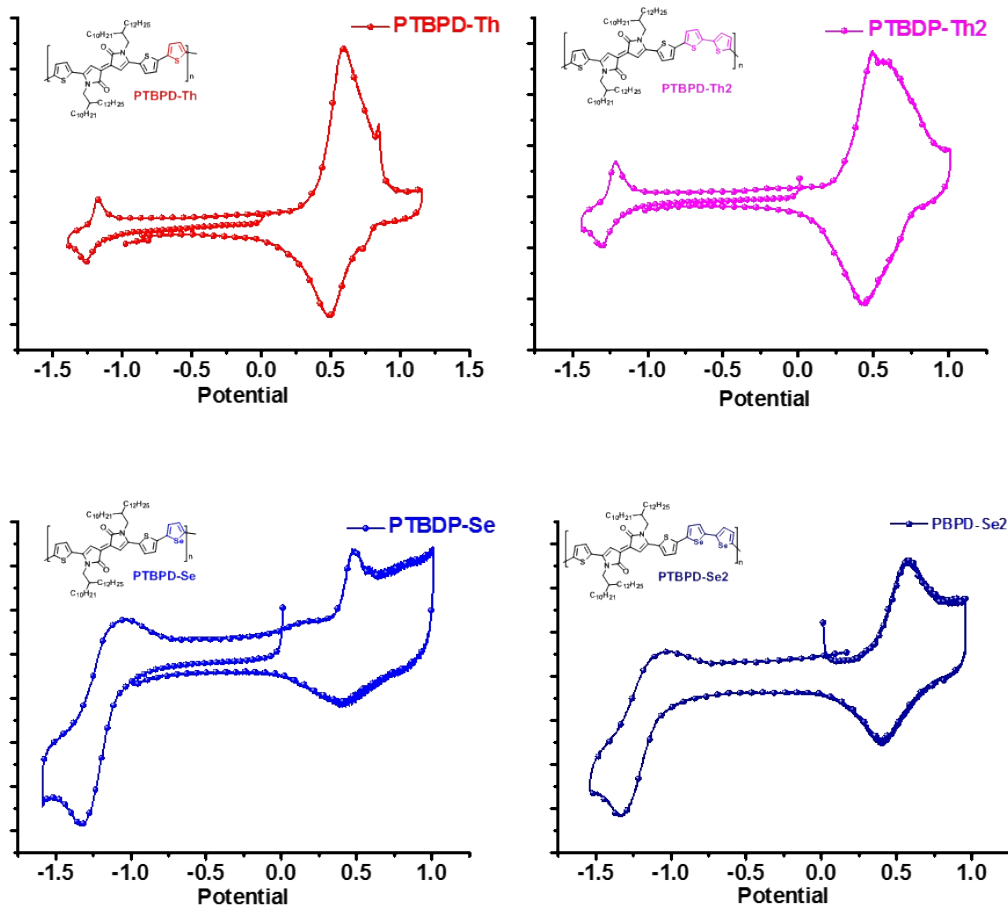


Fig. S9 Cyclic voltammety of TBBDP-based polymers.

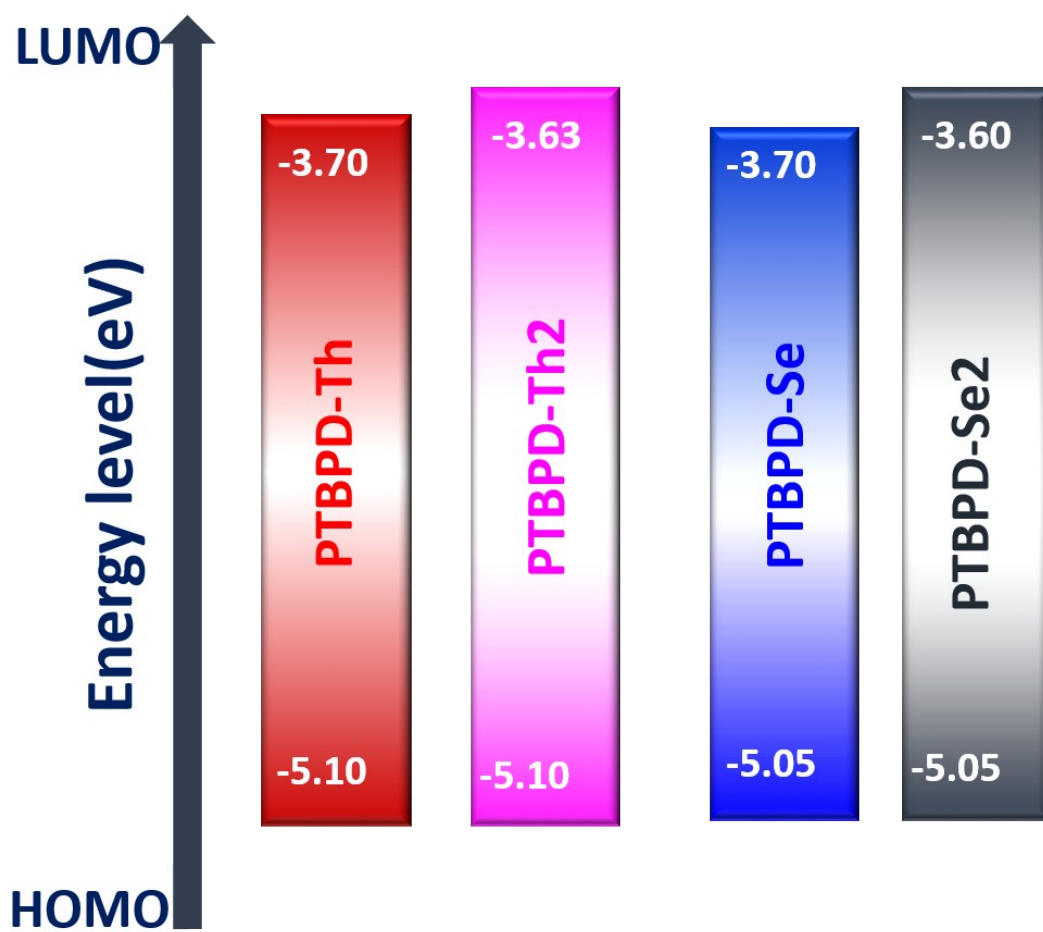
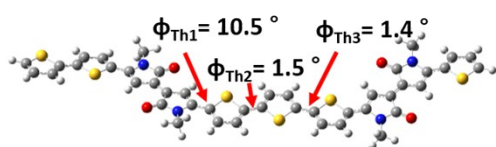
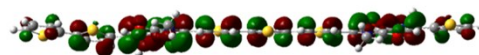


Fig. S10 Energy level diagrams of TBDP-based polymers

PTBPD-Th

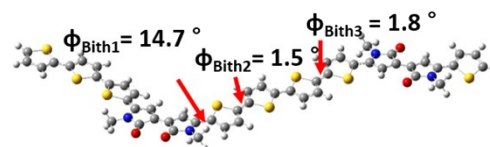


LUMO

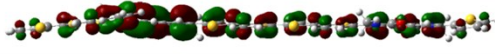


HOMO

PTBPD-Th2

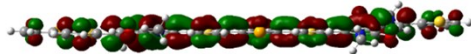
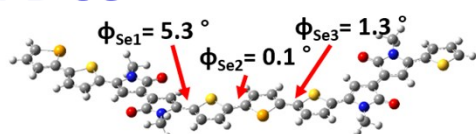


LUMO



HOMO

PTBPD-Se

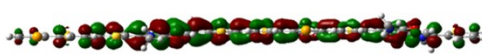
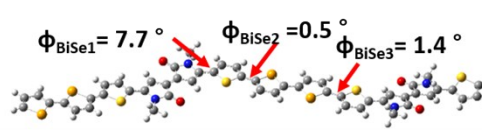


LUMO



HOMO

PTBPD-Se2



LUMO



HOMO

Fig. S11 DFT calculation for TBDP-based polymers with each dimer model at the B3LYP/6-31G* level.

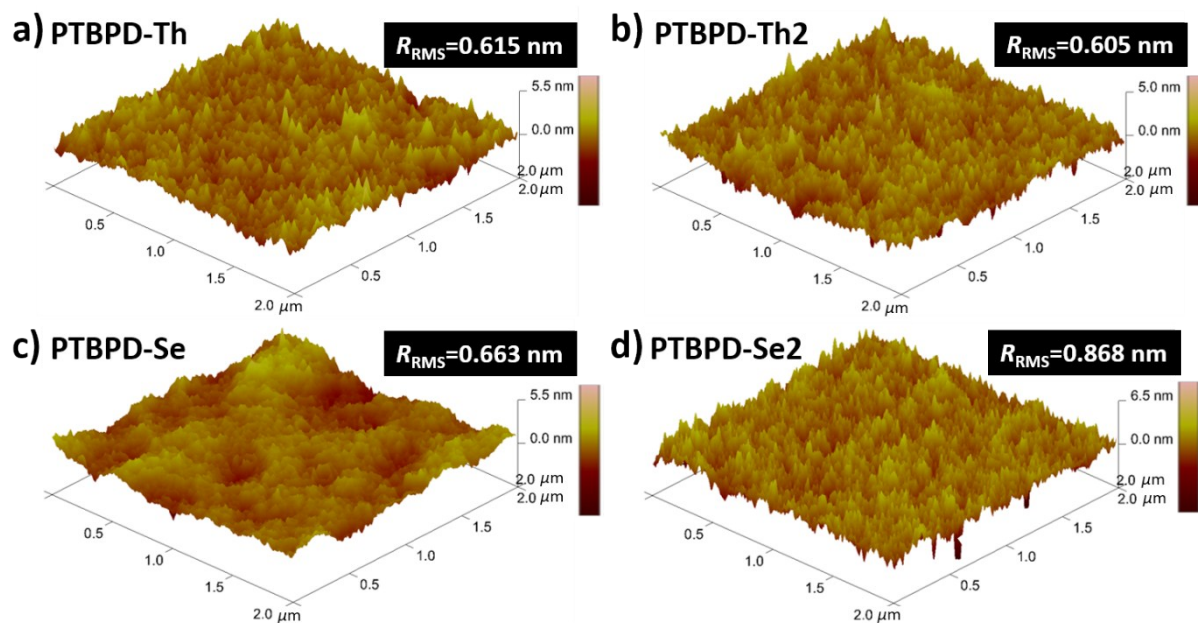


Fig. S12 AFM height images of TBPD-based polymer films annealed at 200 °C: (a) PTBPD-Th, (b) PTBPD-Th2, (c) PTBPD-Se, and (d) PTBPD-Se2.

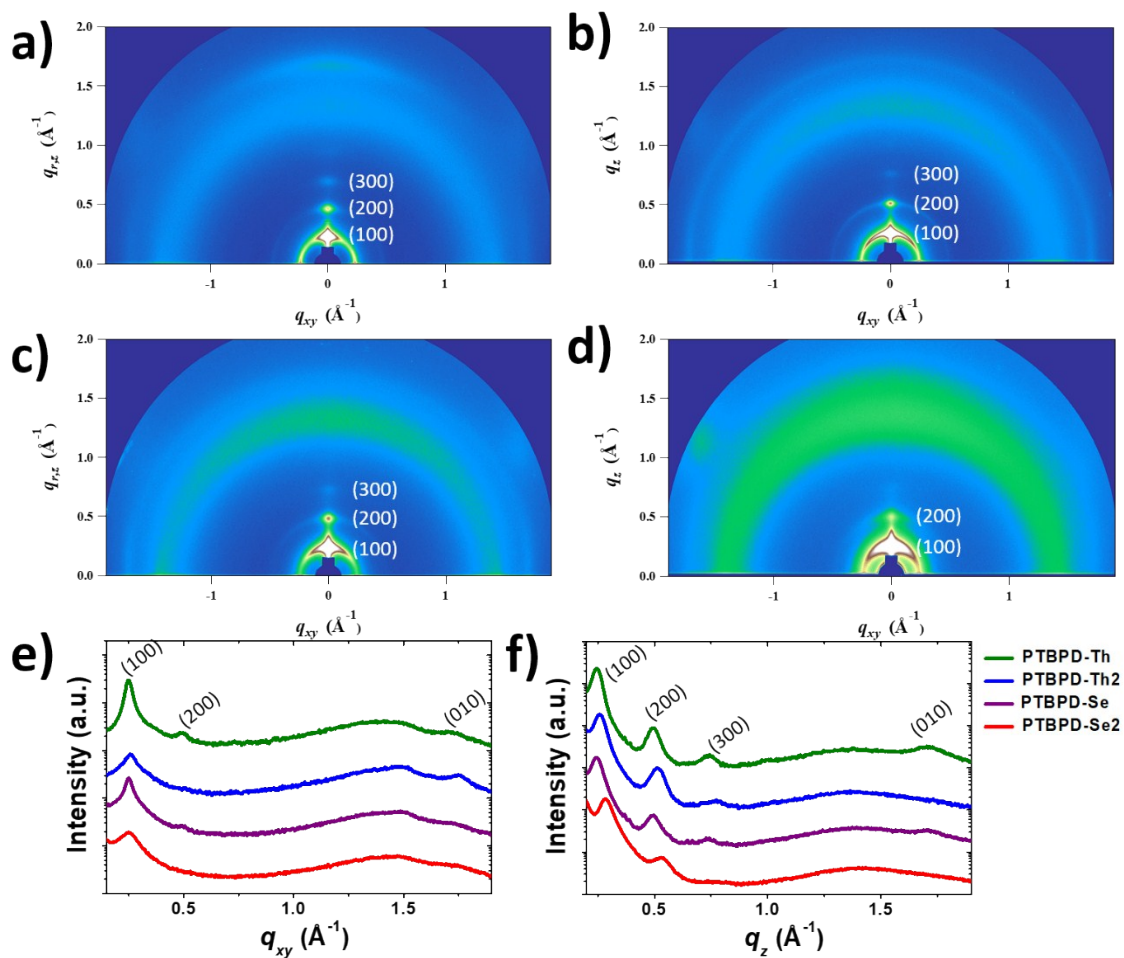


Fig. S13 2D-GIXD images of TBPD-based polymer films without thermal treatment: (a) PTBPD-Th, (b) PTBPD-Th2, (c) PTBPD-Se, and (d) PTBPD-Se2. The corresponding GIXD diffractogram profiles: (e) in-plane and (f) out-of-plane GIXD patterns.

Table S1 Crystallographic parameters of as-cast TBPD-based polymer films

Polymer	Lamellar spacing				π - π spacing	
	q_z [\AA^{-1}]	d [\AA]	L_c [\AA]	L_c/d	q_{xy} [\AA^{-1}]	d [\AA]
PTBPD-Th	0.246	25.6	142.0	5.55	1.72	3.66
PTBPD-Th2	0.260	24.2	128.8	5.32	1.75	3.59
PTBPD-Se	0.245	25.6	142.3	5.55	— ^a	— ^a
PTBPD-Se2	0.285	22.0	121.8	5.53	— ^a	— ^a

^aNot detected

Table S2 Summary of FET performance of solution sheared non-annealed TBPD polymer films.

Polymer ^a	$\mu_{h,max}^b$ [cm ² V ⁻¹ s ⁻¹]	$\mu_{h,avg}^c$ [cm ² V ⁻¹ s ⁻¹]	I_{on}/I_{off}^d	V_T^e [V]
PTBPD-Th	0.25	0.13 (± 0.093) ^f	$> 10^4$	18.1
PTBPD-Th2	0.022	0.010 (± 0.047)	$> 10^5$	14.2
PTBPD-Se	0.040	0.027 (± 0.012)	$> 10^4$	19.7
PTBPD-Se2	0.083	0.049 (± 0.015)	$> 10^5$	18.9

^aThe FET performance of solution sheared non-annealed polymer films fabricated with 3 mg mL⁻¹ of 1,2-dichlorobenzene solution; ^bThe maximum and ^caverage mobility of the FET devices ($L = 50 \mu\text{m}$ and $W = 1000 \mu\text{m}$); ^dThe on- and off-current ratio; ^eThe average threshold voltage; ^fThe standard deviation.

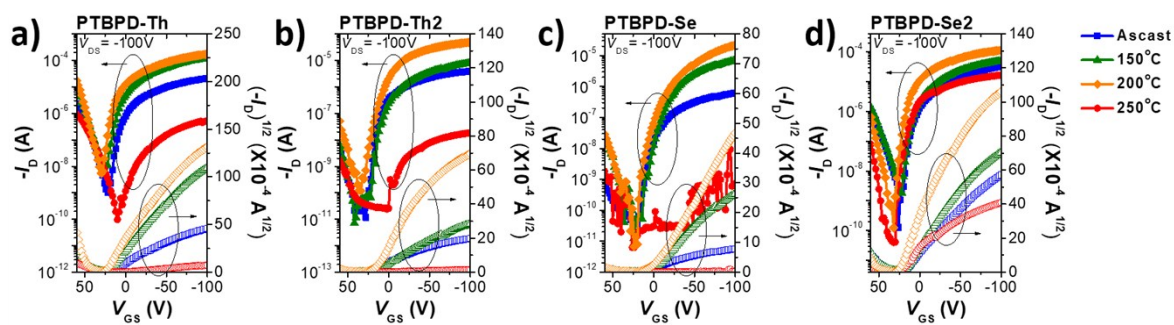


Fig. S14 Transfer characteristics obtained from TBPD-based polymer films before (blue) and after thermal treatment at various annealing temperature of 150 °C (green), 200 °C (orange), and 250 °C (red): (a) PTBPD-Th, (b) PTBPD-Th2, (c) PTBPD-Se, and (d) PTBPD-Se2.

Table S3 FET performance of TBPD polymer films fabricated using various solvents.

Condition		<i>p</i> -channel			
Polymer ^a	Solvent ^b	$\mu_{h,max}^c$ [cm ² V ⁻¹ s ⁻¹]	$\mu_{h,avg}^d$ [cm ² V ⁻¹ s ⁻¹]	I_{on}/I_{off}^e	V_T^f [V]
PTBPD-Th	CB	0.30	0.25 (± 0.034) ^g	$> 10^3$	15.7
	DCB	0.46	0.37 (± 0.066)	$> 10^4$	14.7
PTBPD-Th2	CB	0.030	0.026 (± 0.0031)	$> 10^6$	15.0
	DCB	0.12	0.10 (± 0.012)	$> 10^5$	11.2
PTBPD-Se	CB	0.015	0.010 (± 0.0021)	$> 10^5$	-1.3
	DCB	0.11	0.066 (± 0.029)	$> 10^5$	25.5
PTBPD-Se2	CB	0.087	0.070 (± 0.012)	$> 10^5$	8.6
	DCB	0.28	0.22 (± 0.044)	$> 10^5$	17.5

^aThe FET performance of solution sheared polymer films annealed at 200 °C was tested in a nitrogen atmosphere;

^bThe polymer films were fabricated with 3 mg mL⁻¹ chlorobenzene and 1, 2-dichlorobenzene solution; ^cThe maximum and ^daverage mobility of the FET devices ($L = 50 \mu\text{m}$ and $W = 1000 \mu\text{m}$); ^eThe on- and off-current ratio;

^fThe average threshold voltage; ^gThe standard deviation.

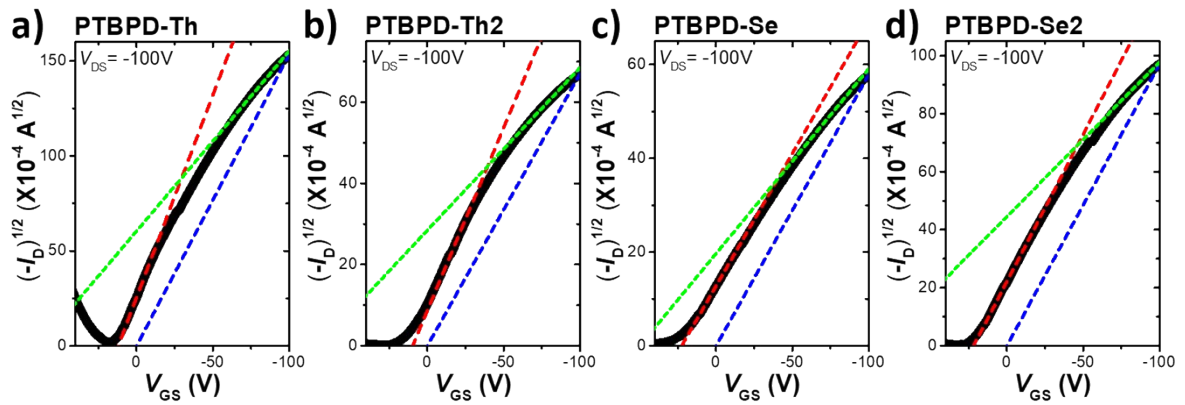


Fig. S15 Transfer curves with three fitting lines obtained from TBPD-based polymer films after thermal treatment at 200 °C: (a) PTBPD-Th, (b) PTBPD-Th2, (c) PTBPD-Se, and (d) PTBPD-Se2. The red line represents the fitting line of the maximum mobility. The green line represents the fitting line at a high gate voltage above the kink. The blue line represents the ideal FET characteristics which satisfy the ideal Shockley equations.

Table S4 Summary of the calculated mobilities of TBPD polymer-based OFETs.

Polymer ^a	$\mu_{h,\max}^b$ [cm ² V ⁻¹ s ⁻¹]	μ_{highV}^c [cm ² V ⁻¹ s ⁻¹]	μ_{eff}^d [cm ² V ⁻¹ s ⁻¹]	R_{sat}^e [%]
PTBPD-Th	0.46	0.16	0.15	33.1
PTBPD-Th2	0.12	0.032	0.048	39.5
PTBPD-Se	0.11	0.061	0.067	63.4
PTBPD-Se2	0.31	0.14	0.15	48.4

^aThe FET performance of solution sheared polymer films fabricated with 3 mg mL⁻¹ of 1,2-dichlorobenzene solution was tested in a nitrogen atmosphere; ^bThe maximum mobility of the FET devices; ^cThe mobility obtained from the high gate voltage region; ^dThe effective mobility ($\mu_{\text{eff}} = \mu_{\text{max}} \times R_{\text{sat}}$); ^eThe reliability factor.

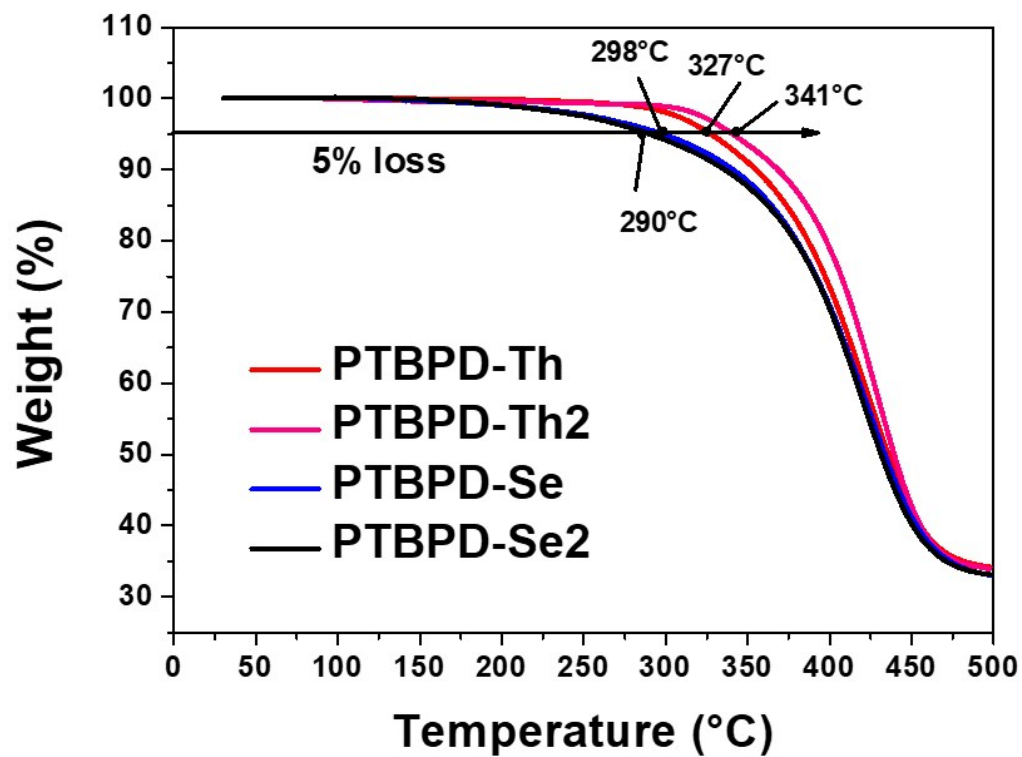


Fig. S16. Thermogravimetric analysis (TGA) of all polymers.

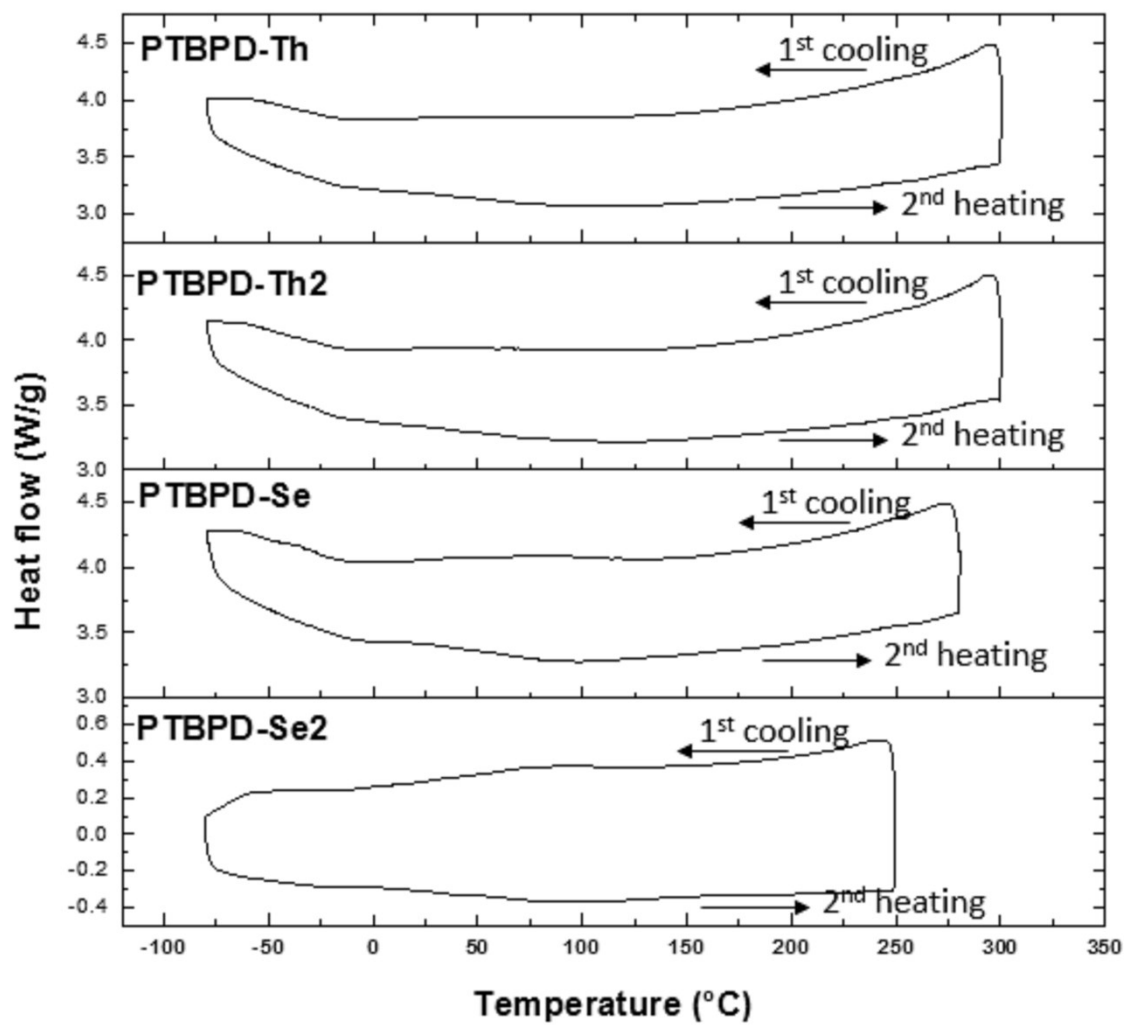


Fig. S17 The differential scanning calorimetry (DSC) data of all polymers.